A fast and efficient method for the analysis of α-dicarbonyl compounds in aqueous solutions: development and application

Nicolas Brun, Juan Miguel González-Sánchez, Carine Demelas, Jean-Louis Clément, Anne Monod

A fast and efficient method for the analysis of α-dicarbonyl compounds in aqueous solutions: development and application

Nicolas Brun[1,2], Juan Miguel González-Sánchez[1,2,3], Carine Demelas[1], Jean-Louis Clément[2], Anne Monod[1]

[1]Aix Marseille Univ, CNRS, LCE, Marseille, France
[2]Aix Marseille Univ, CNRS, ICR, Marseille, France
Now at [3]Aix Marseille Univ, CNRS, MIO, Marseille, France

Correspondence to: Nicolas Brun (nicolas.brun@univ-amu.fr) and Anne Monod (anne.monod@univ-amu.fr)

Keywords: analytical chemistry, atmospheric chemistry, fogs and clouds chemistry, α-dicarbonyls, High-Performance Ion Chromatography

Abstract.

Among the highly oxygenated species formed *in situ* in the atmosphere, α-dicarbonyl compounds are the most reactive species, thus contributing to the formation of secondary organic aerosols that affect both air quality and climate. They are ubiquitous in the atmosphere and are easily transferred to the atmospheric aqueous phase due to their high solubility. In addition, α-dicarbonyl compounds are toxic compounds found in food in biochemistry studies as they can be produced endogenously through various pathways and exogenously through the Maillard reaction. In this work, we take advantage of the high reactivity of α-dicarbonyl compounds in alkaline solutions (intramolecular Cannizzaro reaction) to develop an analytical method based on high performance ion chromatography. This fast and efficient method is suitable for glyoxal, methylglyoxal and phenylglyoxal which are detected as glycolate, lactate and mandelate anions respectively, with 100% conversion at pH > 12 and room temperature for exposure times to hydroxide ranging from 5 minutes to 4 h. Diacetyl is detected as 2,4-dihydroxy-2,4-dimethyl-5-oxohexanoate due to a base catalysed aldol reaction that occurs before the Cannizzaro reaction. The analytical method is successfully applied to monitor glyoxal consumption during aqueous phase HO· oxidation, an atmospherically relevant reaction using concentrations that can be observed in fog and cloud water. The method also reveals potential analytical artifacts that can occur in the use of ion chromatography for α-hydroxy carboxylates measurements in complex matrices due to α-dicarbonyl conversion during the analysis time. An estimation of the artifact is given for each of the studied α-hydroxy carboxylates. Other polyfunctional and pH-sensitive compounds that are potentially present in environmental samples (such as nitrooxycarbonyls) can also be converted into α-hydroxy carboxylates and/or nitrite ions within the HPIC run. This shows the need for complementary analytical measurements when complex matrices are studied.

1. Introduction

Fast and efficient analysis of small α-dicarbonyl compounds is essential for atmospheric chemistry, biochemistry and food chemistry as these compounds are highly reactive, toxic and ubiquitous in the environment. In the atmosphere, α-dicarbonyl compounds such as glyoxal, methylglyoxal and diacetyl, are primary and secondary highly reactive compounds. They are abundant in the gas, aqueous, and particulate phases. They are produced by the gas-phase oxidation of anthropogenic aromatic hydrocarbons (Volkamer et al., 2001; Calvert et al., 2002; Sato et al., 2012), biogenic terpenes and isoprene (Saunders et al., 2003; Miller et al., 2016; Wennberg et al., 2018) and can potentially originate from marine biogenic fatty acids (Chiu et al., 2017). Alpha-dicarbonyl compounds have a high effective Henry's law constant driven by hydrate (gem-diol) formation (Boreddy and Hoffmann, 1988; Sander, 2015). Therefore, although highly volatile, they partition into the atmospheric aqueous phase (liquid water droplets and/or wet aerosols), where they undergo a specific reactivity that is very different from that in the gas phase, the latter being dominated by direct photolysis. Among the most ubiquitous α-dicarbonyls, glyoxal and methylglyoxal aqueous-phase reactivity leads to the formation of low- or semi-volatile compounds: they can form oligomers *via* hemiacetalisation (Loeffler et al., 2006; Avzianova and Brooks, 2013), acid-catalysed aldol condensation (de Haan et al., 2009a; Nozière et al., 2010) and/or photo-oxidation (Tan et al., 2009; Lee et al., 2011; Zhao et al., 2012). They can be oxidised to oxalic acid, the dominant dicarboxylic acid in the atmosphere, often observed as the most abundant organic species in particle matter (Carlton et al., 2007; Tan et al., 2010; Boreddy and Kawamura, 2018). Although the reactivity of diacetyl in the atmosphere has been much less studied, it has been shown to form light-absorbing products *via* aqueous-phase reactions with ammonia and/or amines, like glyoxal and methylglyoxal (de Haan et al., 2009b; Kampf et al., 2012; Powelson et al., 2014; Laskin et al., 2015; Li et al., 2021; Jimenez et al., 2022; Zhang et al., 2022; Faust et al., 1997; Kampf et al., 2016; Grace et al., 2020). From all these studies, α-dicarbonyl compounds are likely important atmospheric precursors of Secondary Organic Aerosols (SOA) that affect both air quality and climate.

Alpha-dicarbonyl compounds are also of major interest in food and biochemistry due to their toxicity: they can be generated endogenously and exogenously (Lange et al., 2012). In food, the Maillard reaction occurs between reducing sugars and amino acids and produces various α-dicarbonyl compounds including glyoxal, methylglyoxal and diacetyl (Cha et al., 2019). Previous studies reveal that α-dicarbonyls are also precursors of heterocyclic flavour chemicals in the Maillard reaction (Wang and Ho, 2012; Jiang et al., 2013); α-dicarbonyl compounds have been found in fermented food, dairy products and beverages (Degen et al., 2012; Wang et al., 2017; Kim et al., 2021). *In vivo*, glyoxal can be formed through various pathways, including autoxidation of carbohydrates and ascorbate, degradation of glycated proteins and lipid peroxidation (Lange et al., 2012). In addition, α-dicarbonyl compounds can modify proteins and form advanced glycation end products, which are related to the development of many chronic diseases (Lange et al., 2012; Poulsen et al., 2013; Svendsen et al., 2016; Ansari et al., 2018). Finally, α-dicarbonyl compounds are cytotoxic and inhibit the function of human enzymes responsible for DNA repair (Amoroso et al., 2013).

Due to their high reactivity, quantitative measurements of α-dicarbonyl compounds are challenging in aqueous samples. Indeed, carbonyl compounds promptly hydrate in water, forming gem-diols that are not detectable by spectrophotometry. Except for diacetyl which can be detected by UV-Visible absorption due to its low hydration in the aqueous phase (Faust et al., 1997; Zuman, 2002), there are currently no methods for the direct detection and quantification of these compounds in the liquid phase. The most widely employed methods for the analysis of these compounds use amino trapping reagents to convert α-dicarbonyl compounds into more stable imine derivative chromophores and/or fluorophores that can be quantified by High-Performance Liquid Chromatography (HPLC) or Gas Chromatography (GC) coupled to UV detection, fluorimetry or Mass Spectrometry (MS) (see SI1). The 3 most common amino trapping reagents ((2,3,4,5,6-pentafluorobenzyl)hydroxylamine (PFBHA), 2,4-dinitrophenylhydrazine (DNPH) and o-phenylenediamine) trap α-dicarbonyl compounds to produce oximes, hydrazones and quinoxalines, respectively. However, amino trapping reagents show some disadvantages for the analysis of α-dicarbonyl compounds. Undesirable formation of mono-derivatives has been reported (Nakajima et al., 2007). Moreover, double derivatisation is generally slower than single derivatisation and leads to the formation of three or four isomers (depending on the symmetry of the α-dicarbonyl compound). For these reasons, derivatisation using a di-amino compound such as o-phenylenediamine appears to be more suitable for efficient trapping of α-dicarbonyl compounds. Furthermore, although some of the amino trapping reagents are very expensive, they are used in large excess to favour the derivatisation reaction. The trapping reagents must then be accurately separated from the imine derivatives for quantification. In addition, the pH of the reaction must be carefully controlled because water elimination in the derivatisation reaction is acid-catalysed but is also reversible under acidic conditions (Layer, 1963). A too low pH, the reaction can also lead to competitive aldol condensation of α-dicarbonyl compounds. Finally, imine derivatives can be poorly water-soluble, affecting the derivatisation in the case of aqueous solutions.

In this work, a specific method based on High-Performance Ion Chromatography (HPIC) was developed for a simple, fast and accessible analysis of α-dicarbonyl compounds in aqueous solutions. The method has the advantages of high selectivity, high sensitivity, and simple equipment requirement (Chen et al., 2005). The analytical conditions and performances set by Chen et al. (2005) for glyoxal were revisited and complemented by MS detection. The method was extended to other α-dicarbonyl compounds. Methylglyoxal and diacetyl were selected as they are ubiquitous in the environment, and phenylglyoxal was chosen as a proxy for aromatic α-dicarbonyl compounds formed in atmospheric SOA. The developed method was successfully applied to glyoxal monitoring during its aqueous phase HO·-oxidation under atmospherically realistic conditions. The paper discusses the advantages of the method as well as potential analytical artifacts that can occur using HPIC for α-hydroxy carboxylate measurements in complex aqueous environmental samples.

2 Materials and methods

The method is based on converting α-dicarbonyl compounds into α-hydroxy carboxylates in the presence of a strong base *via* a benzilic acid rearrangement, an intramolecular disproportionation that derives from the Canizzaro reaction (Selman, S., & Eastham, 1960; Fratzke and Reilly, 1986; Burke and Marques, 2007). The reaction consists of HO^- addition, C-C rotation, carbanion migration, and proton relay towards the produced anions (Fig. 1). The formed α-hydroxy carboxylates can then be easily detected using HPIC coupled with conductivity detection and/or mass spectrometry. The chemical conversion can be performed either by addition of a strong base in the sample before analysis, or into the HPIC system using the mobile phase with an appropriate NaOH concentration as reagent. In the latter, the measurement of α-dicarbonyl compounds can be performed without any conversion process before the analysis and thus allows for direct measurement, but with significantly lower performances than the former, as shown in the results.

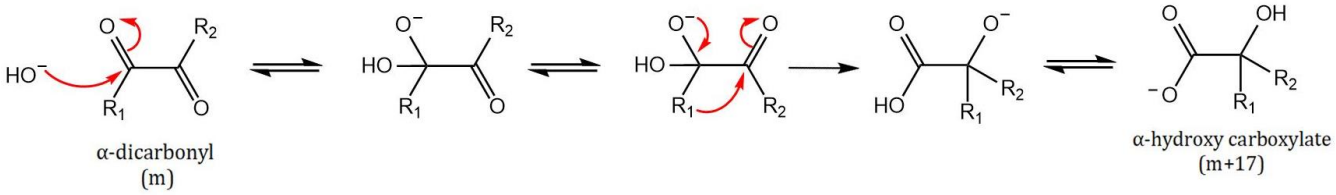

Fig. 1 – General scheme of the chemical conversion of α-dicarbonyl compounds to α-hydroxy carboxylates in an alkaline solution (adapted from Yamabe et al., 2006). Each step is reversible, except for the carbanion migration (3rd step), which is the rate determining step.

2.1 Instrumental setup and operating conditions

Carboxylates were analysed and quantified by two HPIC systems equipped with different mobile phases. The first one was a Dionex ICS-3000 High-Performance Ion Chromatograph driven by Chromeleon® software. The HPIC was coupled with a Dionex CD25 Conductivity Detector (CD) in parallel with a Dionex surveyor MSQ mass spectrometer. In each analysis, the samples were automatically injected using a 100 µL injection loop into a Dionex IonPac AG11-HC precolumn (4 x 50 mm) connected to a Dionex IonPac AS11-HC column (4 x 250 mm) thermostated at 30 °C with a particle size of 9 µm. The HPIC was equipped with a Dionex ACRS 500 chemical suppressor with a constant flow of 50 mM H_2SO_4 at 3.5 mL min^{-1}. The MSQ mass spectrometer was operated in electrospray ionization (ESI) negative mode under a desolvation gas flow of 6 L min^{-1} at 600 °C and a capillary voltage of 3.5 kV. The sample cone voltage was set at 35 V and carboxylates were detected and quantified as their deprotonated molecules ($[M-H]^-$) with simultaneous full scan and Selected Ion-Monitoring (SIM) for the targeted α-hydroxy carboxylates. In each sample, 1 mg L^{-1} of valeric acid was employed as an internal standard. The injection volume was 100 µL and the flow rate was 1 mL min^{-1}. The mobile phase consisted of an aqueous NaOH solution degassed with purified He and kept under N_2 atmosphere during the analyses. The separation was performed by isocratic elution. Several tests were performed using various NaOH concentrations in the mobile phase, ranging from 17.5 to 45 mM (pH range = 12.24 - 12.65), to accelerate the conversion of α-dicarbonyl compounds within the chromatographic column. This system is further designated as $HPIC_{NaOH}$.

The second HPIC system used comprised a less alkaline mobile phase to study the effect of the mobile phase pH on the analytical performances. For this purpose, a 761 Compact HPIC System from Metrohm AG was employed including a Metrosep A Supp 4 (4 x 250 mm) column with a particle size of 5 µm. The system comprised a conductivity detector and a suppressor module running at a constant flow of 0.5 mL min^{-1} of 20 mM H_2SO_4. Samples were manually injected using a 20 µL injection loop. The entire HPIC system was thermostated at 20 °C. At a flow rate of 1 mL min^{-1}, an isocratic method with a single eluent consisting of an aqueous solution of 2 mM $NaHCO_3$ and 1.3 mM Na_2CO_3 (pH = 10.14) was used. This system is further designated as $HPIC_{carbonate}$.

2.2 Chemicals and sample preparations

All chemicals were commercially available and used as supplied as listed in SI2, except for α-nitrooxyacetone that was synthesised following a protocol described in SI3. Conversions of α-dicarbonyl compounds in alkaline solutions were performed either into the HPIC system using the mobile phase as reagent (further designated as method A), or before analysis in amber vials by addition of 17.5 mM NaOH followed by manual shaking for 10 seconds (further designated as method B), as summarised in Fig. **2**. The analyses were systematically complemented with blanks including the UHQ water used for dilutions, the NaOH solutions used for the conversion reactions and valeric acid as internal standard. Conversion kinetics experiments were performed using $HPIC_{NaOH}$ by repeatedly sampling the same vials after an initial NaOH addition (at pH = 12.24) and manual shaking for 10 seconds.

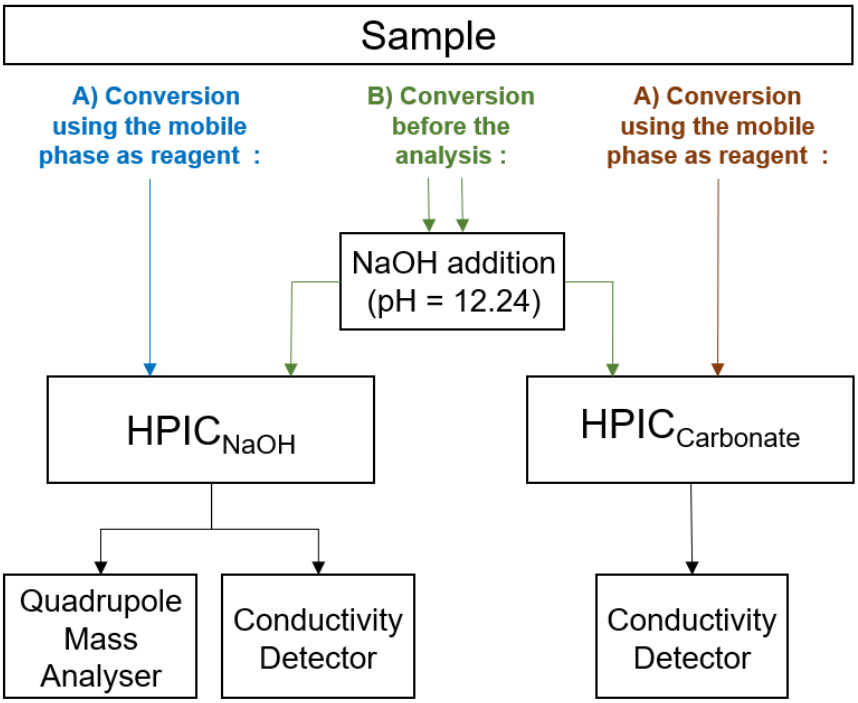

Fig. 2 – **Summary diagram of the various analytical conditions investigated. Samples were converted either using the mobile phase as reagent (method A) or before the analysis (method B) and analysed either by HPIC$_{NaOH}$ or by HPIC$_{Carbonate}$.**

2.3 Aqueous photooxidation

The study of glyoxal HO·-oxidation in the aqueous phase was performed applying the analytical method developed. The reaction was performed in a 450 mL batch reactor equipped with Pyrex double wall thermostated at 25°C with ethylene glycol and covered by a quartz lid. The reactor was irradiated by a Xenon arc lamp 1000 W (LOT Quantum Design) to mimic the solar irradiance (see SI4). Radiations below 290 nm were filtered by an AM1.5 standard filter (ASTM 892). Homogeneity of the solution was ensured by magnetic stirring.

HO· radicals were generated by H_2O_2 photolysis. In this experiment, H_2O_2 was monitored by UHPLC-UV analysis (see SI5), pH and dissolved O_2 were continuously monitored in the solution using specific probes (C3020, Consort, and FDO925, WTW, respectively). Aliquots were sampled at regular times in amber vials, which quenched the photolysis reaction. Glyoxal and carboxylate products were analysed from the samples using HPIC$_{NaOH}$. For glyoxal analysis, the samples were five times diluted and converted before analysis using method B, as described in section 2.2. The photooxidation experiments were performed at a glyoxal initial concentration of 100 µM, about twice higher than the maximum amounts of glyoxal or methylglyoxal observed in clouds and fogs (Li et al., 2020; Ervens et al., 2013). The initial H_2O_2 concentration (1 mM) was chosen to favor by more than 80 % the HO· reaction towards glyoxal over its reaction with H_2O_2. A series of control experiments were performed using HPIC$_{NaOH}$: i) dark reaction of H_2O_2 with glyoxal (previously reported by Zhao et al., 2012), ii) direct photolysis of glyoxal (without H_2O_2), and iii) direct photolysis of H_2O_2 (without glyoxal).

3 Results and discussions

3.1 Method development

Conversion of α-dicarbonyl compounds into α-hydroxy carboxylates through benzilic acid rearrangement is an irreversible reaction occurring in alkaline medium (Fig. 1) that is highly sensitive to pH (Selman, S., & Eastham, 1960; Gill, 1991; Yamabe et al., 2006; Wang, 2010). The influence of pH on the analytical method (using HPIC$_{carbonate}$ and HPIC$_{NaOH}$) was first studied in details for glyoxal (in sub-section 3.1.1), then it was applied to methyglyoxal, phenyglyoxal and diacetyl (sub-section 3.1.2). For each compound, the conversion kinetics were investigated, as well as their conversion proportions (sub-section 3.1.3). The analytical performances of the method are finally presented in sub-section 3.1.4.

3.1.1 Optimisation of glyoxal analysis

Using method A, no conversion of glyoxal to glycolate was observed using HPIC$_{carbonate}$ in contrast to the results obtained using HPIC$_{NaOH}$. As shown in Fig. 3 a strong glycolate signal was observed using a highly alkaline mobile phase. These results

are in very good agreement with the kinetic model of Fratzke and Reilly (1986) which predicts complete conversion of glyoxal in the analysis timescale (10 min) at pH = 12.24 (conversion half-life of glyoxal < 10 s, see SI6). Glyoxal measurements can therefore be performed using $HPIC_{NaOH}$ without any conversion process before the chromatographic analysis, thus allowing its direct measurement. However, under these conditions, glycolate quantification was complicated by low-quality chromatograms due to large peak tailing (Fig. 3). This phenomenon can be explained by the reaction medium successive conditions encountered by the sample in the HPIC. The reaction started as soon as the sample was in contact with the mobile phase in the injection loop. When the sample entered the HPIC column, the early formed glycolate molecules were retained, while the unconverted non-ionic glyoxal molecules were not retained, but were continually converted during the elution process. The reaction was promoted by the exchangeable counterions of the stationary phase. The reaction then also took place at the outlet of the column and up to the chemical suppressor where the pH was lowered thus stopping the reaction. Ranging from 17.5 to 45 mM NaOH concentration as $HPIC_{NaOH}$ mobile phase (pH range = 12.24 – 12.65) the asymmetry factor slightly decreased (Fig. 3) as the reaction rate and elution were accelerated. Nevertheless, the glycolate peak asymmetry factor was much lower and closer to 1 using method B and $HPIC_{NaOH}$ (Fig. 3).

Using method B and $HPIC_{carbonate}$, a glycolate signal was also observed showing the irreversibility of the reaction. However, the strong OH^- signal due to the high NaOH concentration in the sample and the unsuitable suppressor conditions overlapped the glycolate signal and resulted in a low-quality chromatogram (not shown).

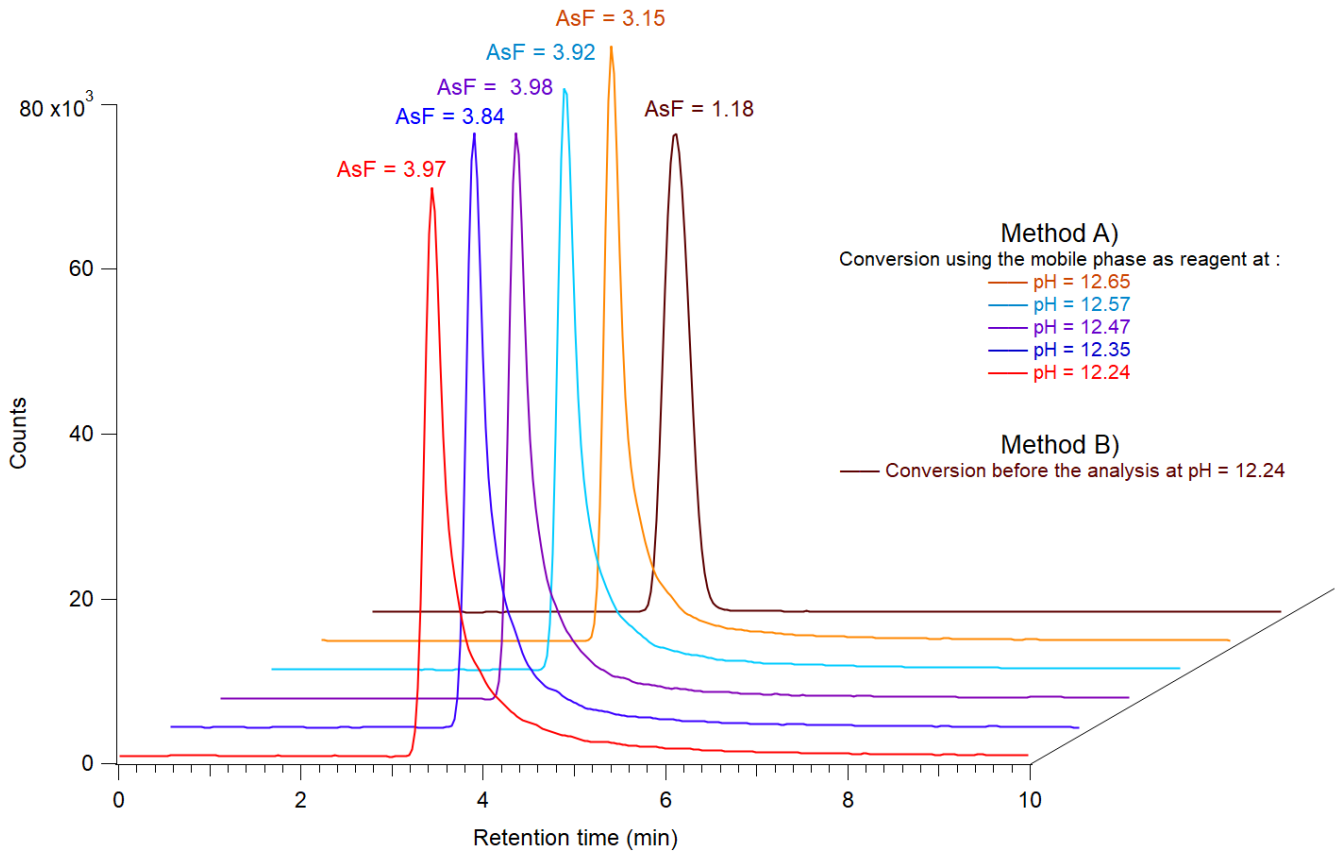

Fig. 3 – $HPIC_{NaOH}$ SIM chromatograms at m/z = 75 of a 5 µM glyoxal solution using either method B (conversion before the analysis at pH 12.24), or method A (conversion using the mobile phase as reagent), at various NaOH concentrations, corresponding to the indicated pH. The peak asymmetry factors (AsF) are indicated at the top of each peak with the corresponding colors. The asymmetry factor was calculated at 10% of the peak height.

3.1.2 Application to other α-dicarbonyl compounds

Using method A, as observed for glyoxal, no chemical conversion of methylglyoxal and phenylglyoxal was obtained using $HPIC_{carbonate}$, but a strong signal of conversion was observed using $HPIC_{NaOH}$. Under these conditions, lactate and mandelate were detected respectively for methylglyoxal and phenylglyoxal, as expected from the mechanism (Fig. 1). However, in the same manner as for glyoxal, the chromatograms showed large peak tailing and the deformations were solved using method B (Fig. 4). These conversion observations are in very good agreement with the kinetic model predictions of Fratzke and Reilly (1986) and Hine et al. (1971), (conversion half-life of methylglyoxal and phenylglyoxal are 7 and 8 min respectively) as detailed in SI6.

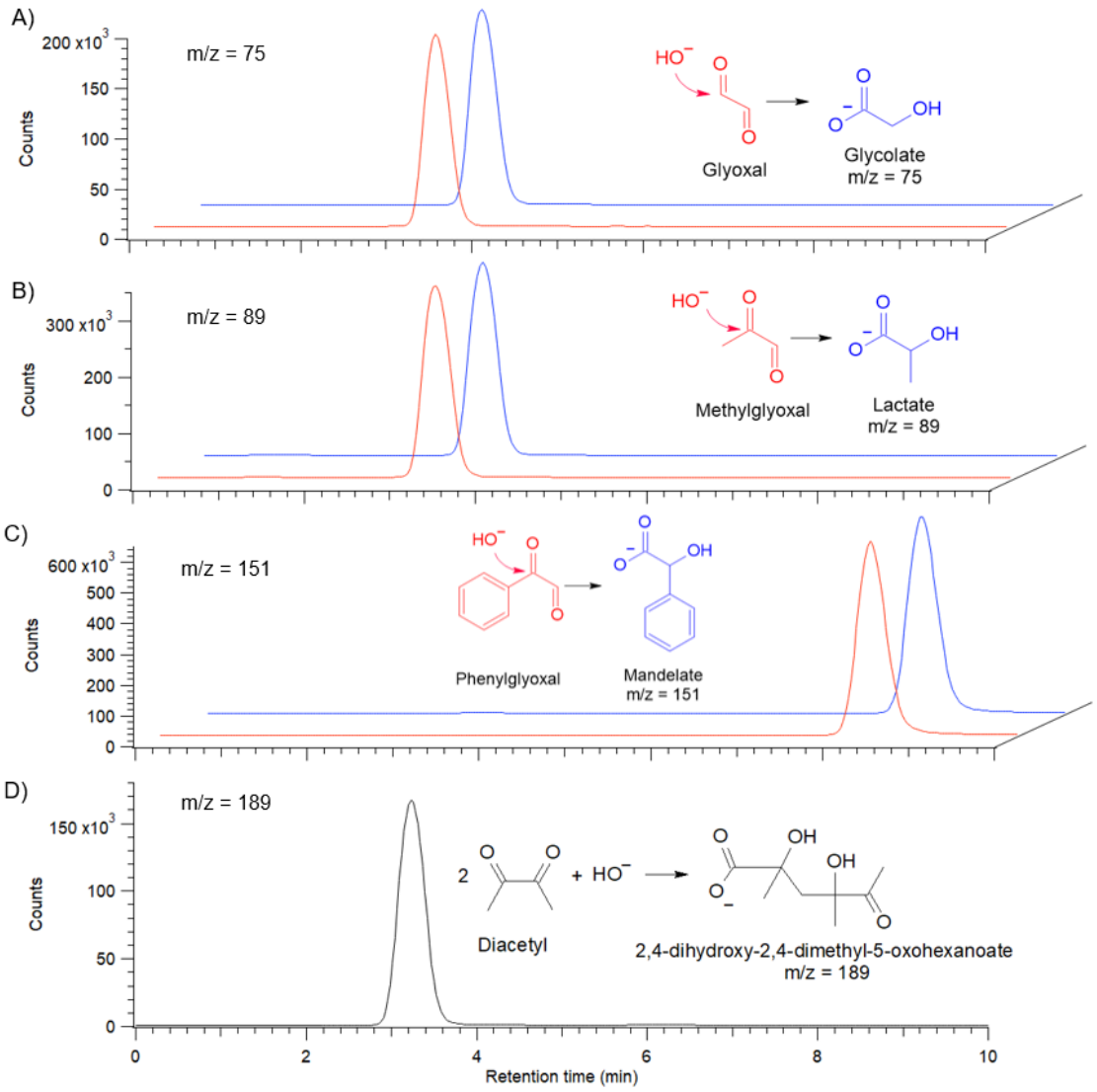

Fig. 4 – HPIC$_{NaOH}$ selected-ion monitoring (SIM) chromatograms A) at m/z = 75 of glyoxal (red) and glycolate (blue) solutions B) at m/z = 89 of methylglyoxal (red) and lactate (blue) solutions C) at m/z = 151 of phenylglyoxal (red) and mandelate (blue) solutions. D) SIM chromatogram at m/z = 189 of a diacetyl solution. The concentration of each compound was 10 µM, the conversion time was 5, 120, 240 and 720 min for glyoxal, methylglyoxal, phenylglyoxal and diacetyl, respectively.

Concerning diacetyl, no signal was detected at m/z = 103 which corresponds to 2-methyllactate, expected from the mechanism shown in Fig. 1. Instead, a strong signal was observed at m/z = 189 (Fig. 4D) which shows that a more complex chemical process occurs under alkaline conditions. This was explained by an additional mechanism shown in Fig. SI7: diacetyl bears enolisable hydrogens which allow aldol condensation to compete with the benzilic rearrangement. Diacetyl thus undergoes base catalysed aldol condensation and forms an α-dicarbonyl dimer that is converted to 2,4-dihydroxy-2,4-dimethyl-5-oxohexanoate (shown in Fig. 4D) *via* the benzilic acid rearrangement (Machell, 1960). The latter compound is not

commercially available, therefore no quantitative comparison with a standard product could be done. Although methylglyoxal bears enolisable hydrogens on its methyl group as well, no product from a similar mechanism was detected, probably due to its fast conversion kinetics (see next section) and the smaller number of hydrogens in the molecule.

In summary, the chemical conversion measurement method is also applicable to methylglyoxal, phenylglyoxal and diacetyl detected as lactate, mandelate and 2,4-dihydroxy-2,4-dimethyl-5-oxohexanoate, respectively, and is more efficient for quantification using method B than method A.

3.1.3 Conversion kinetics

In addition to being strongly dependent on pH, the conversion kinetics at 25°C were observed to be highly different from one α-dicarbonyl compound to the other as shown in Fig. 5 where they are compared to the kinetic model predictions proposed by Fratzke and Reilly (1986) for glyoxal and methylglyoxal and by Hine et al. (1971) for phenylglyoxal. For glyoxal, the conversion was extremely fast (conversion half-life of glyoxal < 10 s) and reached its maximum within less than 4 minutes. For methylglyoxal, phenylglyoxal and diacetyl, the conversion kinetics were slower (conversion half-life of methylglyoxal, phenylglyoxal and diacetyl was 7 min, 29 min and 2 h, respectively) likely because of the more complex mechanisms of the reaction conversion. In this mechanism (Fig. 1), the migration step of the R_1 group is rate-determining (Yamabe et al., 2006), therefore, the reaction kinetics depend on the nature of the R_1 and/or R_2 groups. Compared to glyoxal, methylglyoxal and phenylglyoxal bear a methyl and a phenyl group, respectively, that probably slows down the conversion reaction by steric hindrance. Furthermore, diacetyl possesses two enolisable methyl groups which allow for more competitive aldol condensation kinetics. In this case, the conversion reaction occurs after the dimerisation step 1 (Fig. SI7), which likely explains the globally slower kinetics. Therefore, in addition to low-quality chromatograms, method A results in incomplete conversion of α-dicarbonyl compounds with slow conversion kinetics (for methylglyoxal, phenylglyoxal and diacetyl) and thus much lower performances.

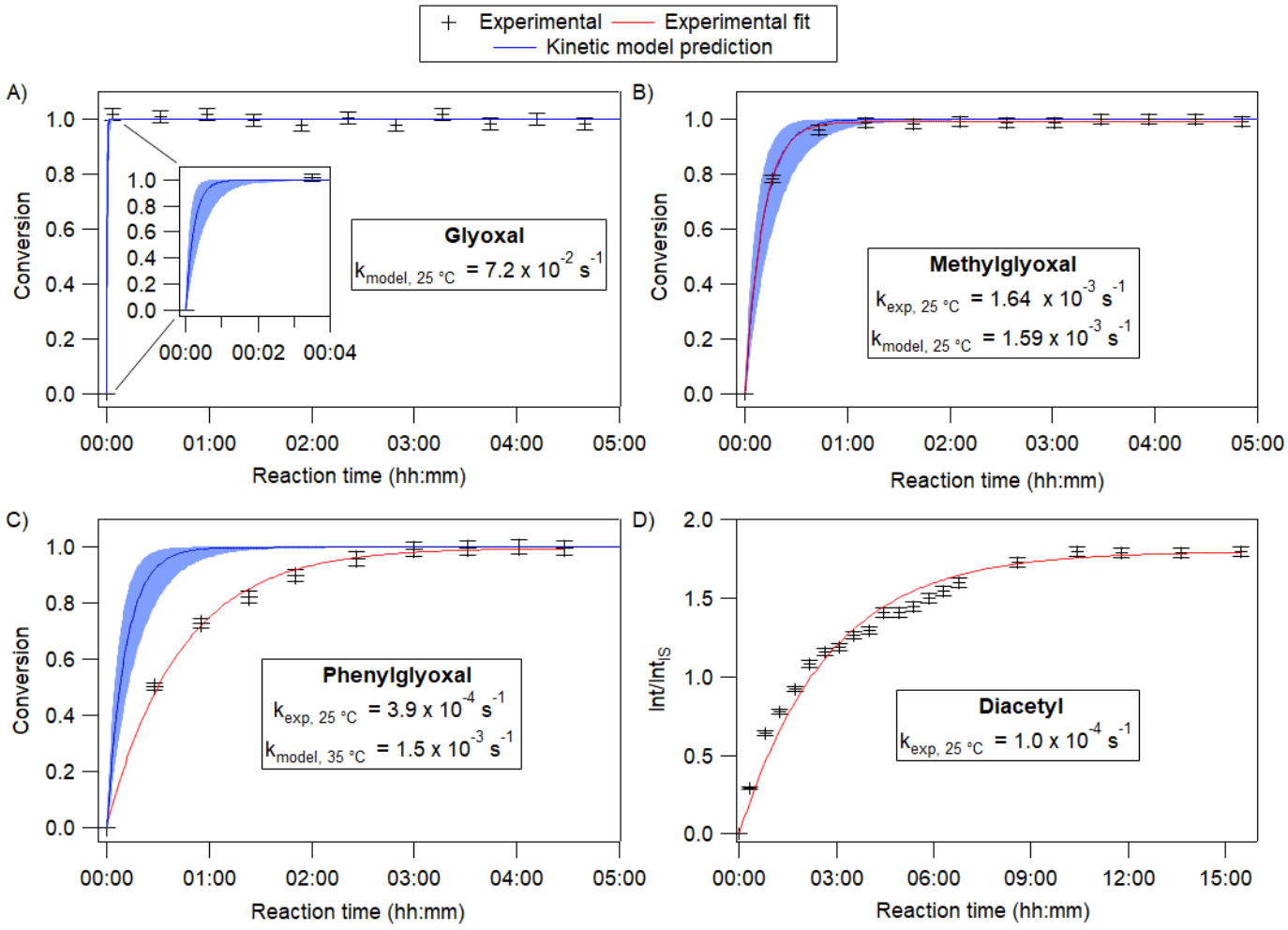

Fig. 5 – Temporal evolution of the conversion of A) glyoxal to glycolate (the inner graph shows a zoom in the first 4 minutes), B) methylglyoxal to lactate, C) phenylglyoxal to mandelate and D) diacetyl to 2,4-dihydroxy-2,4-dimethyl-5-oxohexanoate using SIM at m/z = 75, 89, 103 and 151, respectively. Chromatographic peak integrated areas (Int) were normalised to integrated areas of valerate, the internal standard (Int_{IS}) and compared to the signal of the corresponding α-hydroxy carboxylate, when possible, to compute the chemical conversion. Experimental error bars represent the standard deviation between triplicates. Red lines are the experimental fit using pseudo first-order kinetics: 1-exp(-kt). Blue lines (and shaded blue areas) show the kinetic model prediction at pH = 12.2 (± 0.2) set by Fratzke et al. (1986) for glyoxal and methyglyoxal and by Hine et al. (1971) for phenylglyoxal.

Fig. 5 shows that all the experimental kinetics are first-order, in very good agreement with the kinetic results by Hine et al. (1971) and Fratzke and Reilly (1986). Using exponential fits, pseudo first-order conversion rate constants of methylglyoxal, phenylglyoxal, and diacetyl were respectively $k_{exp,\ methylglyoxal} = 1.6\times10^{-3}\ s^{-1}$, $k_{exp,\ phenylglyoxal} = 3.9\times10^{-4}\ s^{-1}$, $k_{exp,\ diacetyl} = 1.0\times10^{-4}\ s^{-1}$. These values are compared in Fig. 5 to the kinetic model predictions developed by Fratzke and Reilly (1986) and Hine et al. (1971) that predict k as a function of pH (see SI6). Although no rate constant of glyoxal conversion could be determined in this work due to its very fast kinetics under our experimental conditions, Fig. 5 shows excellent agreements between our kinetic results and those predicted by Fratzke and Reilly (1986) for glyoxal and methylglyoxal at 25°C. A significantly slower kinetics

is observed for phenylglyoxal when compared to the kinetic model prediction by Hine et al. (1971) that was established at 35 °C only. The temperature effect probably explains the kinetic differences observed. Assuming an Arrhenius dependence of the pseudo first order rate constant of glyoxal conversion and from the work of Fratzke and Reilly (1986), the activation energy of the glyoxal conversion is 61.2 kJ mol^{-1} at pH = 12.24 (see SI8). A rough estimation of the activation energy of the conversion of phenylglyoxal at pH = 12.24 using the value obtained by Hine et al. (1971) at 35 °C and our rate constant determined at 25 °C results in an activation energy of approximately 100 kJ mol^{-1}. Although this value is a rough estimation and should be confirmed by more experimental data at various temperatures, it is significantly higher than that of glyoxal and may be explained by steric hindrance due to the phenyl group of the phenylglyoxal.

3.1.4 Analytical method performances

The performances were evaluated from the optimal pH and kinetics conditions for each compound using method B, i.e. conversion before analysis into amber vials at pH > 12 for 5 minutes to 12 h and MS analysis using $HPIC_{NaOH}$. The resulting SIM chromatograms are shown in Fig. 4. The reaction yield was determined, when possible, at the end of the reaction by comparison of the α-hydroxy carboxylate signal in the converted α-dicarbonyl samples and the signal of authentic α-hydroxy carboxylate standard samples, using the two HPIC systems. The performances obtained for the four α-dicarbonyl compounds are shown in Table 1. For glyoxal, methylglyoxal and phenylglyoxal the yields were higher than 97 %, whereas no conversion yield could be derived for diacetyl due to the lack of standard of 2,4-dihydroxy-2,4-dimethyl-5-oxohexanoate. The peak area of each α-hydroxy carboxylate showed a good linearity (R^2 > 0.99) using concentrations of the corresponding α-dicarbonyl compounds ranging from 0.1 to 20 µM (see SI9) with good reproducibility (variation coefficient < 2.5 %). No interaction was observed in mixture samples of the four α-dicarbonyls and the same values as in single samples were recovered. The detection limits for the four α-dicarbonyls ranged from 9 nM to 66 nM (determined using Signal/Noise = 3) and are of the same order as other recently published results using traditional derivatisation measurement methods (Rodigast et al., 2015). Glyoxal and methylglyoxal show average concentrations in cloud and fog water ranging respectively from 0.6 to 96 µM and from 0.3 to 93 µM (Ervens et al., 2013; Li et al., 2020). The method developed in this work thus presents the performances needed by environmental samples and has the advantage of being simple and fast.

α-dicarbonyl			Detected α-hydroxy carboxylate			Analytical performances				
Name	m/z	Structure	Name	m/z	Structure	Yield of the conversion reaction (reaction time)	Linearity (R^2)	Sensitivity (μM^{-1})	Detection limit (nM)	Variation coefficient between triplicates
Glyoxal	58		Glycolate	75		100 ± 4 % (5 min)	0.9969	0.13	33	2.3%
Methylglyoxal	72		Lactate	89		97 ± 5 % (2 hrs)	0.9985	0.31	43	1.7%
Phenylglyoxal	134		Mandelate	151	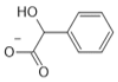	101 ± 5 % (4 hrs)	0.999	1.16	9	2.5%
Diacetyl	86		2,4-dihydroxy-2,4-dimethyl-5-oxohexanoate	189	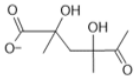	not determined	0.9984	0.2	66	1.9%

Table 1 – Analytical performances of $HPIC_{NaOH}$ analysis of α-dicarbonyl compounds after chemical conversion to α-hydroxy carboxylate anions in NaOH solutions at pH>12 (method B).

3.2 Application to aqueous phase photooxidation of glyoxal

The chemical conversion method for α-dicarbonyl analysis shows good performances, is simple, fast and requires simple instrumentation and cheap solvents. This makes it very suitable for laboratory studies on specific α-dicarbonyl compounds such as aqueous glyoxal ·OH-oxidation. The results (Fig. 6) show that control experiments revealed no significant direct photolysis of glyoxal in the aqueous phase, as expected from glyoxal hydration that supresses the carbonyl groups and leads to the reversible formation of gem-diol, with a high hydration equilibrium constant reached within less than a second (hydration half-life of glyoxal is < 0.1 seconds as compiled by Ervens and Volkamer, 2010). This reaction thus prevents the radiation absorption by the molecule in water (Montoya and Mellado, 1994). The reaction between glyoxal and H_2O_2 reported previously (Zhao et al., 2012) was not observed under our experimental conditions, probably due to our low initial concentrations that slowed down the formation of hydroxyhydroperoxides. In the presence of $HO^\bullet$ radicals (produced from H_2O_2 + hν), glyoxal concentrations decreased exponentially by one order of magnitude within 7h of reaction, while H_2O_2 concentrations decreased by a factor of 11% (SI10). These kinetics allowed us to derive some values of the rate constants of the limiting reactions, i.e. H_2O_2 direct photolysis J_{H2O2}, and glyoxal $HO^\bullet$ oxidation k_{OH}. Assuming steady state concentrations for $HO^\bullet$ and $HO_2^\bullet$ radicals, the glyoxal and H_2O_2 concentration time profiles were simulated using the Microsoft® Excel® Solver routine. Both J_{H2O2}, and k_{OH} were optimized to minimize the sum of the square differences between calculated and experimental data (see SI10). The results show a good agreement between the simulated and the experimental concentrations (Fig. 6 and SI10), and a value of $k_{OH} = 1.07 \times 10^9$ M^{-1} s^{-1} was derived. Although this value is a rough estimation due to the steady state approximations, it is in good agreement with the values of 1.1×10^9 and 0.92×10^9 M^{-1} s^{-1} determined by Buxton et al. (1997) and Schaefer et al. (2015) respectively. The main photooxidation reaction product detected was secondary oxalic acid, in agreement with previous studies (Tan et al., 2009; Lee et al., 2011; Lim et al., 2013; Schaefer et al., 2015). The measurement method developed in this work

has thus proven to be simple and efficient to monitor glyoxal during a reaction of atmospheric interest, under concentrations similar to those observed in clouds and fogs.

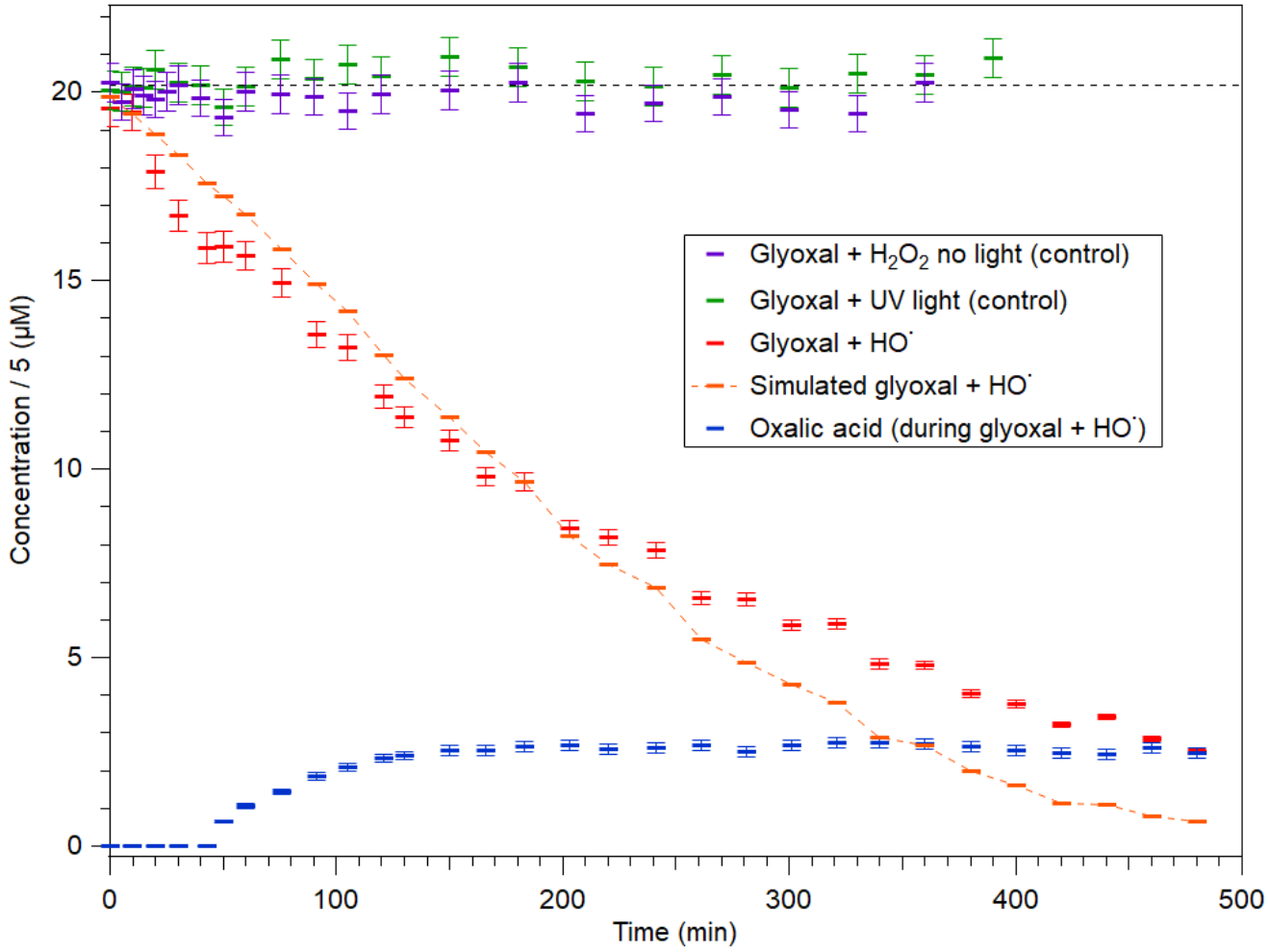

Fig. 6 – Experimental and simulated glyoxal time profiles during its aqueous phase reaction using SIM at m/z = 75 (glycolate). At m/z = 89 oxalate was also monitored as the main secondary reaction product. Error bars represent the standard deviation between analytical triplicates. The samples were diluted by a factor of 5 before analysis.

3.3 Discussions on environmental analysis

The method also shows some disadvantages and should therefore be used with caution, especially for complex environmental samples. Concentrations of α-dicarbonyls may be overestimated if the samples contain the corresponding α-hydroxy carboxylate. In this case, it is necessary to perform a preliminary α-hydroxy carboxylate quantification at lower pH, to prevent the conversion of any α-dicarbonyl compound (see SI11 for more details). For this reason, the method is more suitable for targeted laboratory studies but remains applicable to environmental samples.

Our results also show that the presence of α-dicarbonyl compounds can induce overestimation biases especially when looking for organic acids and carboxylates in environmental samples. To evaluate the importance of the conversions that may occur, a simple calculation was performed for the two most abundant α-dicarbonyl compounds, glyoxal and methylglyoxal. Considering the kinetics model proposed by Fratzke and Reilly (1986) and our results, using a typical HPIC method (Wang, 2009) whose pH gradient is often used for environmental analysis, up to 24 and 3% of glyoxal and methylglyoxal can be converted to their corresponding hydroxy carboxylates respectively. However, the induced biases on the quantification of α-hydroxy carboxylates depend on the relative abundance of α-dicarbonyl to α-hydroxy carboxylate concentrations in the sample. Note that other α-dicarbonyl compounds can also interfere with gluconate, malate, 2-hydroxyvalerate, mucate, tartarate, citrate and isocitrate measurements. Specific analyses should thus be performed using our methodology (i.e. $HPIC_{NaOH}$ and $HPIC_{carbonate}$) to determine the importance of these biases in environmental samples.

Other pH-sensitive compounds can be converted into α-dicarbonyls and hydroxy-carboxylates during HPIC analysis using highly alkaline mobile phases, especially compounds prone to base-catalysed hydrolysis. For example, seeking for any contaminants during the synthesis of α-nitrooxyacetone, large quantities of lactate and nitrite were detected using $HPIC_{NaOH}$ (see Fig. 7 and SI12 for chromatographic conditions). This phenomenon was explained by the prompt base-catalysed hydrolysis of α-nitrooxyacetone that produced nitrite ions and methylglyoxal which was then converted into lactate during the $HPIC_{NaOH}$ analysis (see the mechanism in Fig. 7). Particular care should therefore be taken when performing routine HPIC analysis of environmental samples which likely contain polyfunctional and pH-sensitive compounds, especially for the measurement of glycolate, lactate and nitrite ions.

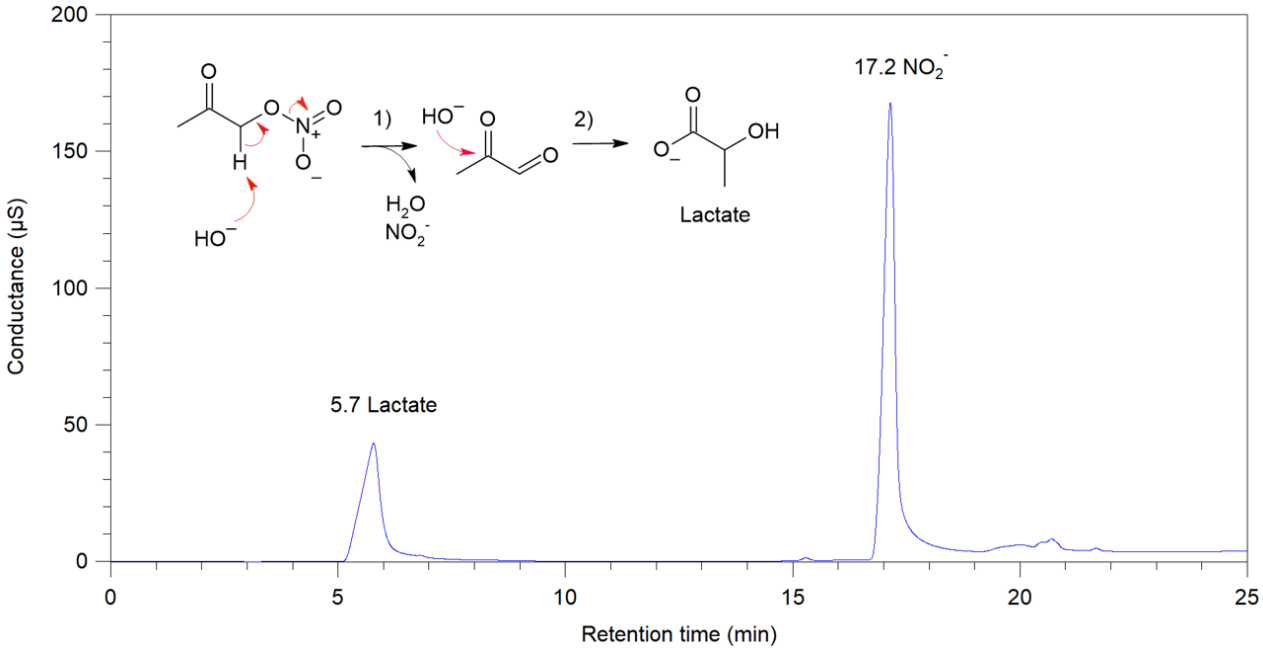

Fig. 7 $HPIC_{NaOH}$ chromatogram of an aqueous solution of α-nitrooxyacetone. In the figure: Reaction mechanism of α-nitrooxyacetone in alkaline medium. 1) Basic hydrolysis 2) Benzilic acid rearrangement.

4. Conclusions

In this work, we took advantage of the high reactivity of α-dicarbonyl compounds in alkaline solutions (intramolecular Cannizzaro reaction) to develop an analytical method based on HPIC. The chemical conversion can be performed in the sample before analysis or in the HPIC system during elution using the mobile phase as reagent. The required mobile phase pH depends on the targeted α-dicarbonyl compound, the analysis time and the temperature of the HPIC system. However, when the chemical conversion was performed using the mobile phase as reagent, chromatographic distortions were observed under our analytical conditions that were solved by performing the chemical conversion before analysis. When the chemical conversion was performed before analysis, the analytical method performances were comparable to other recently published traditional derivatisation methods and allowed for laboratory experiments, such as aqueous phase HO·-oxidation of glyoxal, to be conducted in concentration ranges similar to those observed in the atmosphere. Compared to the previous derivatisation methods, this alkaline chemical conversion method is much simpler, faster and cheaper but is more suitable for targeted laboratory experiments. Indeed, potential interferences of α-hydroxy carboxylates in complex environmental samples can occur, they need to be treated with caution, for example, using two different elution methods, i.e. midly alkaline eluents such as carboxylates and highly alkaline eluents such as sodium or potassium hydroxide solutions.

Acknowledgements

The authors acknowledge the support from the French National Research Agency (ANR-PRCI) through the projects PARAMOUNT (ANR18-CE92-0038-02) and AEROFOG (ANR-22-CE92-0051) and Doctorate school ED251 "Environmental sciences". The authors would like to thank their colleagues from the laboratory LCE at Aix-Marseille University, Robert DI ROCCO, who helped with the $HPIC_{carbonate}$ analysis, and Etienne Quivet who helped on the choice of the Journal for paper submission.

References

Amoroso, A., Maga, G., Daglia, M., 2013. Cytotoxicity of α-dicarbonyl compounds submitted to in vitro simulated digestion process. Food. Chem. 140(4), 654–659, https://doi.org/10.1016/j.foodchem.2012.10.063

Ansari, N. A., Chaudhary, D. K., Dash, D., 2018. Modification of histone by glyoxal: Recognition of glycated histone containing advanced glycation adducts by serum antibodies of type 1 diabetes patients. Glycobiology. 28(4), 207–213, https://doi.org/10.1093/glycob/cwy006.

Avzianova, E., Brooks, S. D., 2013. Raman spectroscopy of glyoxal oligomers in aqueous solutions. Spectro. Acta A, 101, 40–48, https://doi.org/10.1016/j.saa.2012.09.050.

Betterton, E. A., Hoffmann, M. R., 1988. Henry's law constants of some environmentally important aldehydes. Environ. Sci. Technol. 22(12), 1415-1418.

Boreddy, S. K. R., Kawamura, K., 2018. Investigation on the hygroscopicity of oxalic acid and atmospherically relevant oxalate salts under sub- and supersaturated conditions. Environ. Sci. Process. Impacts, 20(7), 1069–1080, https://doi.org/10.1039/c8em00053k

Burke, A., Marques, C., 2007. Mechanistic and Synthetic Aspects of the Benzilic Acid and Ester Rearrangements. Mini-Rev. Org. Chem. 4(4), 310–316, https://doi.org/10.2174/157019307782411707

Buxton, G., Malone, T., Arthur Salmon, G., 1997. Oxidation of glyoxal initiated by OH in oxygenated aqueous solution. J. Chem. Soc., Faraday Transactions, 93(16), 2889-2891.

Calvert, J. G., Atkinson, R., Becker, K. H., Kamens, R. M., Seinfeld, J. H., Wallington, T. H., Yarwood, G., 2002. The mechanisms of atmospheric oxidation of the aromatic hydrocarbons. Oxford University Press, New York.

Carlton, A. G., Turpin, B. J., Altieri, K. E., Seitzinger, S., Reff, A., Lim, H. J., Ervens, B., 2007. Atmospheric oxalic acid and SOA production from glyoxal: results of aqueous photooxidation experiments. Atmos. Environ., 41(35), 7588–7602, https://doi.org/10.1016/j.atmosenv.2007.05.035

Cha, J., Debnath, T., Lee, K. G., 2019. Analysis of α-dicarbonyl compounds and volatiles formed in Maillard reaction model systems. Sci. Rep., 9(1), 1–6, https://doi.org/10.1038/s41598-019-41824-8

Chen, S. P., Huang, T., Sun, S. G., 2005. A new method of ion chromatography technology for speedy determination and analysis in organic electrosynthesis of glyoxylic acid. J. Chromatogr. A, 1089(1-2), 142–147, https://doi.org/10.1016/j.chroma.2005.06.076

Chiu, R., Tinel, L., Gonzalez, L., Ciuraru, R., Bernard, F., George, C., Volkamer, R., 2017. UV photochemistry of carboxylic acids at the air-sea boundary: A relevant source of glyoxal and other oxygenated VOC in the marine atmosphere. Geophys. Res. Lett., 44(2), 1079–1087, https://doi.org/10.1002/2016GL071240

Degen, J., Hellwig, M., Henle, T., 2012. 1,2-Dicarbonyl compounds in commonly consumed foods. J. Agric. Food Chem., 60(28), 7071–7079, https://doi.org/10.1021/jf301306g

Ervens, B., Volkamer, R., 2010. Glyoxal processing by aerosol multiphase chemistry: towards a kinetic modeling framework of secondary organic aerosol formation in aqueous particles. Atmos. Chem. Phys., 10(17), 8219-8244, https://doi.org/10.5194/acp-10-8219-2010

Ervens, B., Wang, Y., Eagar, J., Leaitch, W. R., Macdonald, A. M., Valsaraj, K. T., Herckes, P., 2013. Dissolved organic carbon (DOC) and select aldehydes in cloud and fog water: The role of the aqueous phase in impacting trace gas budgets. Atmos. Chem. Phys., 13(10), 5117–5135, https://doi.org/10.5194/acp-13-5117-2013

Faust, B. C., Powell, K., Rao, C. J., Anastasio, C., 1997. Aqueous-phase photolysis of biacetyl (an α-dicarbonyl compound): A sink for biacetyl and a source of acetic acid, peroxyacetic acid, hydrogen peroxide, and the highly oxidizing acetylperoxyl radical in aqueous aerosols, fogs, and clouds. Atmos. Environ., 31(3), 497–510, https://doi.org/10.1016/S1352-2310(96)00171-9

Fratzke, A. R., Reilly, P. J., 1986. Kinetic analysis of the disproportionation of aqueous glyoxal. Int. J. Chem. Kinet., 18(7), 757–773, https://doi.org/10.1002/kin.550180704

Gill, G. B. (1991). Benzil–Benzilic Acid Rearrangements.

de Haan, D. O., Tolbert, M. A., Jimenez, J. L., 2009a. Atmospheric condensed-phase reactions of glyoxal with methylamine. Geophys. Res. Lett., 36(11), 2–6, https://doi.org/10.1029/2009GL037441

de Haan, D. O., Corrigan, A. L., Tolbert, M. A., Jimenez, J. L., Wood, S. E., Turley, J. J., 2009b. Secondary organic aerosol formation by self-reactions of methylglyoxal and glyoxal in evaporating droplets. Environ. Sci. Technol., 43(21), 8184–8190, https://doi.org/10.1021/es902152t

Hine, J., Koser, G. F., Koser, G. F., 1971. Kinetics and mechanism of the reaction of phenylglyoxal hydrate with sodium hydroxide to give sodium mandelate, 36(23), 3591–3593, https://doi.org/10.1021/jo00822a028

Jiang, Y., Hengel, M., Pan, C., Seiber, J. N., Shibamoto, T., 2013. Determination of toxic α-dicarbonyl compounds, glyoxal, methylglyoxal, and diacetyl, released to the headspace of lipid commodities upon heat treatment. J. Agric. Food. Chem., 61(5), 1067–1071, https://doi.org/10.1021/jf3047303

Jimenez, N. G., Sharp, K. D., Gramyk, T., Ugland, D. Z., Tran, M.-K., Rojas, A., Rafla, M. A., Stewart, D., Galloway, M. M., Lin, P., Laskin, A., Cazaunau, M., Pangui, E., Doussin, J.-F., de Haan, D. O., 2022. Radical-initiated brown carbon formation in sunlit carbonyl–amine–ammonium sulfate ùixtures and aqueous aerosol particles. ACS Earth Space. Chem., 6(1), 228-238, https://doi.org/10.1021/acsearthspacechem.1c00395

Kampf, C. J., Jakob, R., Hoffmann, T., Ho, T., 2012. Identification and characterization of aging products in the glyoxal/ammonium sulfate system – Implications for light-absorbing material in atmospheric aerosols. Atmos. Chem. Phys., 12(14), 6323–6333, https://doi.org/10.5194/acp-12-6323-2012

Kim, Y., Ahn, H., Lee, K. G., 2021. Analysis of glyoxal, methylglyoxal and diacetyl in soy sauce. Food. Sci. Biotechnol., 30(11), 1403–1408, https://doi.org/10.1007/s10068-021-00918-8

Lange, J. N., Wood, K. D., Knight, J., Assimos, D. G., Holmes, R. P., 2012. Glyoxal formation and its role in endogenous oxalate synthesis. Adv. Urol., 2012, 5–10, https://doi.org/10.1155/2012/819202

Laskin, A., Laskin, J., Nizkorodov, S. A., 2015. Chemistry of atmospheric brown carbon. Chem. Rev., 115(10), 4335–4382, https://doi.org/10.1021/cr5006167

Layer, R., 1963. The Chemistry of imines, Chem. Rev., 63, 489–510, https://doi.org/10.1093/litimag/imq040

Lee, A. K. Y., Zhao, R., Gao, S. S., Abbatt, J. P. D., 2011. Aqueous-phase OH oxidation of glyoxal: Application of a novel analytical approach employing aerosol mass spectrometry and complementary off-line techniques. J. Phys. Chem. A, 115(38), 10517–10526, https://doi.org/10.1021/jp204099g

Li, T., Wang, Z., Wang, Y., Wu, C., Liang, Y., Xia, M., Yu, C., Yun, H., Wang, W., Wang, Y., Guo, J., Herrmann, H., Wang, T., 2020. Chemical characteristics of cloud water and the impacts on aerosol properties at a subtropical mountain site in Hong Kong SAR. Atmos. Chem. Phys., 20(1), 391–407, https://doi.org/10.5194/acp-20-391-2020

Li, Y., Ji, Y., Zhao, J., Wang, Y., Shi, Q., Peng, J., Wang, Y., Wang, C., Zhang, F., Wang, Y., Seinfeld, J. H., Zhang, R., 2021. Unexpected oligomerization of small α-dicarbonyls for secondary organic aerosol and brown carbon formation. Environ. Sci. Technol., 55(8), 4430–4439, https://doi.org/10.1021/acs.est.0c08066

Lim, Y. B., Tan, Y., Turpin, B. J., 2013. Chemical insights, explicit chemistry, and yields of secondary organic aerosol from OH radical oxidation of methylglyoxal and glyoxal in the aqueous phase. Atmos. Chem. Phys., 13(17), 8651–8667, https://doi.org/10.5194/acp-13-8651-2013

Loeffler, K. W., Koehler, C. A., Paul, N. M., de Haan, D. O., 2006. Oligomer formation in evaporating aqueous glyoxal and methyl glyoxal solutions. Environ. Sci. Technol., 40(20), 6318–6323, https://doi.org/10.1021/es060810w

Machell, G., 1960. The action of alkali on diacetyl. Journal of the Chemical Society (Resumed), 683–687.

Miller, C. C., Jacob, D., Marais, E., Yu, K., Travis, K., Kim, P., Fisher, J., Zhu, L., Wolfe, G., Keutsch, F., Kaiser, J., Min, K.-E., Brown, S., Washenfelder, R., González Abad, G., Chance, K., 2017. Glyoxal yield from isoprene oxidation and relation to formaldehyde: chemical mechanism, constraints from SENEX aircraft observations, and interpretation of OMI satellite data. Atmos. Chem. Phys., 17(14), 8725-873, https://doi.org/10.5194/acp-17-8725-2017

Montoya, M. R. Mellado, J. M. R., 1994. Use of convolutive potential sweep voltammetry in the calculation of hydration equilibrium constants of α-dicarbonyl compounds. J. Electroanal. Chem, 370(1-2), 183–187, https://doi.org/10.1016/0022-0728(93)03203-2

Nozière, B., Dziedzic, P., Córdova, A., 2010. Inorganic ammonium salts and carbonate salts are efficient catalysts for aldol condensation in atmospheric aerosols. Phys. Chem. Chem. Phys., 12(15), 3864–3872, https://doi.org/10.1039/b924443c

Poulsen, M. W., Hedegaard, R. v., Andersen, J. M., de Courten, B., Bügel, S., Nielsen, J., Skibsted, L. H., Dragsted, L. O., 2013. Advanced glycation endproducts in food and their effects on health. Food chem. toxicol., 60, 10–37, https://doi.org/10.1016/j.fct.2013.06.052

Powelson, M. H., Espelien, B. M., Hawkins, L. N., Galloway, M. M., de Haan, D. O., 2014. Brown carbon formation by aqueous-phase carbonyl compound reactions with amines and ammonium sulfate. Environ. Sci. Technol., 48(2), 985–993, https://doi.org/10.1021/es4038325

Rodigast, M., Mutzel, A., Iinuma, Y., Haferkorn, S., Herrmann, H., 2015. Characterisation and optimisation of a sample preparation method for the detection and quantification of atmospherically relevant carbonyl compounds in aqueous medium. Atmos. Meas. Tech., 8(6), 2409–2416, https://doi.org/10.5194/amt-8-2409-2015

Sander, R., 2015. Compilation of Henry's law constants (version 4.0) for water as solvent. Atmos. Chem. Phys., 15(8), 4399–4981, https://doi.org/10.5194/acp-15-4399-2015

Sato, K., Takami, A., Kato, Y., Seta, T., Fujitani, Y., Hikida, T., Shimono, A., Imamura, T., 2012. AMS and LC/MS analyses of SOA from the photooxidation of benzene and 1,3,5-trimethylbenzene in the presence of NOx: Effects of chemical structure on SOA aging. Atmos. Chem. Phys., 12(10), 4667–4682, https://doi.org/10.5194/acp-12-4667-2012

Saunders, S. M., Jenkin, M. E., Derwent, R. G., Pilling, M. J., 2003. Protocol for the development of the Master Chemical Mechanism, MCM v3 (Part A): Tropospheric degradation of non-aromatic volatile organic compounds. Atmos. Chem. Phys., 3(1), 161–180, https://doi.org/10.5194/acp-3-161-2003

Schaefer, T., van Pinxteren, D., Herrmann, H., 2015. Multiphase chemistry of glyoxal: Revised kinetics of the alkyl radical reaction with molecular oxygen and the reaction of glyoxal with OH, NO3, and SO4- in aqueous solution. Environ. Sci. Technol., 49(1), 343–350, https://doi.org/10.1021/es505860s

Selman, S., & Eastham, J. F., 1960. Benzilic acid and related rearrangements, 14(3), 221–235, https://doi.org/10.1093/nq/s3-IV.94.316-a

Svendsen, C., Høie, A. H., Alexander, J., Murkovic, M., Husøy, T., 2016. The food processing contaminant glyoxal promotes tumour growth in the multiple intestinal neoplasia (Min) mouse model. Food chem. toxicol., 94, 197–202, https://doi.org/10.1016/j.fct.2016.06.006

Tan, Y., Perri, M. J., Seitzinger, S. P., Turpin, B. J., 2009. Effects of precursor concentration and acidic sulfate in aqueous glyoxal - OH radical oxidation and implications for secondary organic aerosol. Environ. Sci. Technol., 43(21), 8105–8112, https://doi.org/10.1021/es901742f

Tan, Y., Carlton, A. G., Seitzinger, S. P., Turpin, B. J., 2010. SOA from methylglyoxal in clouds and wet aerosols: Measurement and prediction of key products. Atmos. Environ., 44(39), 5218–5226, https://doi.org/10.1016/j.atmosenv.2010.08.045

Volkamer, R., Platt, U., Wirtz, K., 2001. Primary and secondary glyoxal formation from aromatics: Experimental evidence for the bicycloalkyl - radical pathway from benzene, toluene, and p-xylene. J. Phys. Chem. A, 105(33), 7865–7874, https://doi.org/10.1021/jp010152w

Wang, C., Lu, Y., Huang, Q., Zheng, T., Sang, S., Lv, L., 2017. Levels and formation of α-dicarbonyl compounds in beverages and the preventive effects of flavonoids. J. Food Sci. Technol., 54(7), 2030–2040, https://doi.org/10.1007/s13197-017-2639-z

Wang, L., 2009. Determination of 32 low molecular mass organic acids in biomass by ion chromatography mass spectrometry.

Wang, Y. Ho, C. T., 2012. Flavour chemistry of methylglyoxal and glyoxal. Chem. Soc. Rev, 41(11), 4140–4149, https://doi.org/10.1039/c2cs35025d

Wennberg, P. O., Bates, K. H., Crounse, J. D., Dodson, L. G., McVay, R. C., Mertens, L. A., Nguyen, T. B., Praske, E., Schwantes, R. H., Smarte, M. D., St Clair, J. M., Teng, A. P., Zhang, X., Seinfeld, J. H., 2018. Gas-phase reactions of isoprene and its major oxidation products. Chem. Rev., 118(7), 3337–3390, https://doi.org/10.1021/acs.chemrev.7b00439

Yamabe, S., Tsuchida, N., Yamazaki, S., 2006. A FMO-controlled reaction path in the benzil-benzilic acid rearrangement. J. Org. Chem., 71(5), 1777–1783, https://doi.org/10.1021/jo051862r

Zhang, R., Gen, M., Liang, Z., Li, Y. J., Chan, C. K., 2022. Photochemical reactions of glyoxal during particulate ammonium nitrate photolysis: brown carbon formation, enhanced glyoxal decay, and organic phase formation. Environ. Sci. Technol., 56(3), 1605–1614, https://doi.org/10.1021/acs.est.1c07211

Zhao, R., Lee, A. K. Y., Abbatt, J. P. D., 2012. Investigation of aqueous-phase photooxidation of glyoxal and methylglyoxal by aerosol chemical ionization mass spectrometry: observation of hydroxyhydroperoxide formation. J. Phys. Chem. A, 116(24), 6253–6263, https://doi.org/10.1021/jp211528d

Zuman, P., 2002. Additions of water, hydroxide ions, alcohols and alkoxide ions to carbonyl and azomethine bonds. Arkivoc, 1, 85–140, https://doi.org/10.3998/ark.5550190.0003.114